

ECOLOGY

Sixty years of plant community change in Europe indicate a shift toward nutrient-rich and denser vegetation

Gabriele Midolo^{1*}, Adam Thomas Clark², Milan Chytrý³, Franz Essl⁴, Stefan Dullinger⁵, Ute Jandt^{6,7}, Helge Bruelheide^{6,7}, Jürgen Dengler^{8,9}, Irena Axmanová³, Svetlana Ačić¹⁰, Olivier Argagnon¹¹, Idoia Biurrun¹², Gianmaria Bonari^{13,14}, Alessandro Chiarucci¹⁵, Renata Čušterevska¹⁶, Pieter De Frenne¹⁷, Michele De Sanctis¹⁸, Jan Divišek³, Jiří Doležal¹⁹, Tetiana Dziuba²⁰, Rasmus Ejrnæs²¹, Emmanuel Garbolino²², Anke Jentsch^{9,23}, Borja Jiménez-Alfaro^{24,25}, Jonathan Lenoir²⁶, Jesper Erenskjold Moeslund²¹, Francesca Napoleone¹⁸, Sabine B. Rumpf²⁷, Jens-Christian Svenning²⁸, Grzegorz Swacha²⁹, Irina Tatarenko³⁰, Martin Večeřa³, Denys Vynokurov^{6,7,20}, Petr Keil¹

Copyright © 2026 The Authors, some rights reserved; exclusive licensee American Association for the Advancement of Science. No claim to original U.S. Government Works. Distributed under a Creative Commons Attribution License 4.0 (CC BY).

Anthropogenic impacts are reshaping plant biodiversity patterns, yet how community-composition shifts track environmental change at large spatial and temporal scales remains unclear. Here, we quantified trends in community-mean plant ecological indicator values (light, temperature, soil moisture, soil nitrogen, and soil reaction) across European vegetation between 1960 and 2020. We used spatiotemporal interpolation based on 644,524 plots and analyzed 18,345 time series encompassing diverse habitats. We found a clear shift in community composition over the past six decades with a steep increase in nitrogen-demanding species across all main habitat types, accompanied by a moderate increase in shade-tolerant species. Forest communities shifted toward species associated with higher soil pH, while wetland communities showed a decline in moisture-dependent species over time. Conversely, temperature indicator values were largely stable, except for recent thermophilization in alpine habitats. Our results indicate a widespread trend toward denser vegetation driven by eutrophication and changes in management practices.

INTRODUCTION

Human activities have directly or indirectly exposed biodiversity to multiple threats, such as climate change and resource exploitation in various parts of the world (1). However, studies focusing on alpha diversity (i.e., local species richness) often reveal no net gain or loss over time across different habitat types (2–6). By contrast, substantial evidence indicates a pronounced temporal turnover in community composition across various ecosystems globally (3, 7), and specifically in European plant communities (8–11). There is well-established evidence that environmental pressures driving these changes include modifications of hydrological regimes (9, 12), nutrient enrichment (specifically nitrogen and phosphorous) (8, 13, 14), global warming (10, 15, 16), alterations in disturbance regimes affecting resources and light availability (9, 14, 17), and changes in soil pH (17–19).

The various environmental pressures driving community change can be revealed through shifts in the prevalence of “indicator species,” i.e., species whose presence is indicative of certain ecological conditions (10, 15, 20, 21). Such a concept is known as “bioindication” (22). Ecological indicator values (EIVs) constitute a well-established expert-based numerical system widely applied for this purpose in Europe (23–25). EIVs classify species based on their mean realized niche position, allowing inference of environmental conditions by averaging the EIVs of co-occurring species at a site (22). Despite EIVs having limitations, such as being frequently correlated and capturing environmental conditions only indirectly, they enable estimates of ecological dimensions where direct measurements are missing. Thus, temporal shifts in species composition within a community enable us to monitor these changes through the lens of bioindication,

¹Department of Spatial Sciences, Faculty of Environmental Sciences, Czech University of Life Sciences Prague, Praha-Suchbát, Czech Republic. ²Department of Biology, University of Graz, Graz, Austria. ³Department of Botany and Zoology, Faculty of Science, Masaryk University, Brno, Czech Republic. ⁴Division of BioInvasions, Global Change and Macroecology, Department of Botany and Biodiversity Research, University of Vienna, Vienna, Austria. ⁵Division of Biodiversity Dynamics and Conservation, Department of Botany and Biodiversity Research, University of Vienna, Vienna, Austria. ⁶Institute of Biology/Geobotany and Botanical Garden, Martin Luther University Halle-Wittenberg, Halle, Germany. ⁷German Centre for Integrative Biodiversity Research (iDiv) Halle-Jena-Leipzig, Leipzig, Germany. ⁸Vegetation Ecology Research Group, Institute of National Resource Sciences (IUNR), Zurich University of Applied Sciences (ZHAW), Wädenswil, Switzerland. ⁹Bayreuth Center of Ecology and Environmental Research (BayCEER), University of Bayreuth, Bayreuth, Germany. ¹⁰Department of Botany, Faculty of Agriculture, University of Belgrade, Serbia. ¹¹Conservatoire Botanique National Méditerranéen, Hyères, France. ¹²Department of Plant Biology and Ecology, Faculty of Science and Technology, University of the Basque Country UPV/EHU, Bilbao, Spain. ¹³Department of Life Sciences, University of Siena, Siena, Italy. ¹⁴National Biodiversity Future Center (NBFC), Palermo, Italy. ¹⁵BIOME Lab, Department of Biological, Geological, and Environmental Sciences, Alma Mater Studiorum, University of Bologna, Bologna, Italy. ¹⁶Faculty of Natural Sciences and Mathematics, Ss. Cyril and Methodius University, Skopje, North Macedonia. ¹⁷Forest and Nature Lab, Faculty of Bioscience Engineering, Ghent University, Ghent, Belgium. ¹⁸Department of Environmental Biology, Sapienza University of Rome, Rome, Italy. ¹⁹Institute of Botany of the Czech Academy of Sciences, Třeboň, Czech Republic. ²⁰Department of Geobotany and Ecology, M.G. Kholodny Institute of Botany, National Academy of Sciences of Ukraine, Kyiv, Ukraine. ²¹Department of Ecoscience, Aarhus University, Aarhus, Denmark. ²²SIGE, MINES Paris PSL, Fontainebleau, France. ²³Disturbance Ecology and Vegetation Dynamics, University of Bayreuth, Bayreuth, Germany. ²⁴Biodiversity Research Institute (IMIB), University of Oviedo-CSIC-Principality of Asturias, Oviedo, Spain. ²⁵Department of Organismal and Systems Biology, University of Oviedo, Oviedo, Spain. ²⁶UMR CNRS 7058 Ecologie et Dynamique des Systèmes Anthropisés (EDYSAN), Université de Picardie Jules Verne, Amiens, France. ²⁷Department of Environmental Sciences, University of Basel, Basel, Switzerland. ²⁸Center for Ecological Dynamics in a Novel Biosphere (ECONOVO), Department of Biology, Aarhus University, Aarhus, Denmark. ²⁹Botanical Garden, University of Wrocław, Wrocław, Poland. ³⁰School of Environment, Earth and Ecosystem Sciences, Open University, Milton Keynes, UK.

*Corresponding author. Email: midolo@fzp.czu.cz

providing insights into the underlying shifts in community-level ecological preferences. For instance, an increasing proportion of warm-adapted species is interpreted as a sign of thermophilization driven by global warming (15, 20). As another example, changes in management practices, such as the cessation of grazing or coppicing (10, 14, 26), often result in an increasing proportion of shade-tolerant species and hence a decrease in the community mean of EIVs for light conditions.

Broad spatiotemporal changes in environmental conditions can thus be reconstructed using bioindication and large-scale vegetation survey data (18). Because the fine-grained reconstruction of past environmental conditions is often impossible, assessing temporal changes in EIVs is especially useful in time series data (21). In addition, EIVs are generally robust to observer-related errors during vegetation resurveys (27). Despite such advantages, large-scale assessments of temporal changes in EIVs are limited by the availability of comprehensive time series of vegetation resurveys. Such data are available in Europe (28), but they are patchy, both spatially and temporally. Thus, we still lack a broad-scale and fine-resolution assessment of how environmental conditions, as indicated by plant community composition, have changed over time across Europe.

To fill this knowledge gap, we here applied a spatiotemporal interpolation (6) using single-survey vegetation-plot data, the most widely available type of data in European vegetation databases (29). In our approach, we treated the community-mean EIVs (CM_{EIVs}) from each one-time survey plot as a single observation in space and time. These observations were then used to fill gaps in the “space-time cube” (30) using machine learning, allowing us to reconstruct their temporal dynamics through model predictions (6). This is feasible due to the inherent spatial and temporal autocorrelation in species occurrences and the environment (31), a feature that tree-based ensemble models can effectively exploit to capture complex interactions and boost the accuracy of site-level predictions.

We aimed to reconstruct how plot-level CM_{EIVs} have changed across Europe and within major habitat types (forests, grasslands, scrub, and wetlands) over the past six decades (1960–2020), enabling comparisons of the direction and magnitude of change. We combined a consensus dataset of European EIV systems for light, temperature, and soil variables (moisture, nitrogen, and reaction), available for 13,874 vascular plant taxa (25), and calculated CM_{EIVs} as the average EIVs of species occurring in each of the 644,524 vegetation-plot records from the European Vegetation Archive (EVA) (29) and ReSurveyEurope (28). We interpolated CM_{EIVs} for each indicator using random forests (32, 33) as a function of space (longitude, latitude, and elevation), time, plot size, and species richness. We also analyzed CM_{EIV} changes over the same period across 57,255 observation records from 18,345 resurvey plots available in ReSurveyEurope and used these data to independently validate our interpolation approach. In Table 1, we detail the expected shifts in EIVs at the community level. We hypothesized these changes to be influenced by various abiotic and biotic characteristics of European habitat types, causing habitat-dependent trends (10, 34, 35). We built our expectations based on several key putative drivers affecting plant community changes, specifically global warming, environmental pollution, and land-use change (Table 1).

RESULTS

Of the five environmental variables assessed as CM_{EIVs} over the past six decades (1960–2020), nitrogen showed the most substantial shift

(Fig. 1). Specifically, we detected a substantial increase in CM_{EIV} for nitrogen across plots (mean change: $+0.25 CM_{EIV}$; Fig. 1A), with 62% of plots increasing by at least 0.1. This trend was consistent across all four habitat types (Fig. 1B) and across Europe (Fig. 2), despite some variation in the magnitude of change in specific habitat types (Fig. 3). Increases in nitrogen values were particularly pronounced in deciduous forests, dry grasslands, and several other scrub and wetland types (Fig. 3). Only a few specific habitats showed either no substantial change (mesic grasslands) or even decreases (wet grasslands, woodland fringes, and tall-forb stands) in nitrogen EIVs.

Although changes in other EIV variables were generally smaller in magnitude, we observed context-dependent trends that varied by habitat type and geographic region. Light availability generally declined over time, showing an opposite trend to nitrogen CM_{EIV} , which suggests that vegetation has become denser and less suitable for light-demanding species. However, the magnitude of change in light was substantially smaller than the change in nitrogen across habitats (mean: $-0.12 CM_{EIV}$). The negative trend for light was most pronounced in grasslands (Fig. 1B) and in wetland habitats for bogs and fens (Fig. 3). In contrast, predictions for forests showed no overall change (Fig. 1B), although coniferous forests exhibited a positive trend and broadleaved evergreen forests a negative one (Fig. 3). Temperature change over time showed low variation across the analyzed plots, with most exhibiting minimal change close to zero across all habitats (Fig. 1A). Nonetheless, a small but detectable increase in CM_{EIV} for temperature was observed in forests (Fig. 1B). In addition, CM_{EIV} for temperature clearly increased in some specific habitats, particularly in alpine and subalpine scrub and grasslands over the past two decades (Fig. 3). Moisture CM_{EIV} declined substantially across wetlands (mean 1960–2020 change: $-0.20 CM_{EIV}$), with pronounced negative trends particularly in helophyte beds ($-0.06 CM_{EIV}$ per decade; table S1). Conversely, moisture CM_{EIV} increased in some dry, nutrient-poor habitats, such as dry grasslands and Mediterranean scrub vegetation, but also in periodically exposed shores (Fig. 3). A generally negative, albeit weak, trend in CM_{EIV} for reaction was observed in grasslands and wetlands overall (Fig. 1B). In contrast, a positive trend was detected in forests and in specific habitats typically associated with more acidic conditions, including tundra, bogs, and fen scrub (Fig. 3). The predicted CM_{EIV} changes for finer habitat types [European Nature Information System (EUNIS) level 2 habitats] were linked to their baseline levels, except for the nitrogen indicator (fig. S1).

The results obtained from spatiotemporal interpolation were consistent with the overall direction of change of CM_{EIVs} estimated from time series data available across Europe (Fig. 4). We found that CM_{EIV} for nitrogen consistently increased in all habitat types with time, accompanied by a consistent decrease in CM_{EIV} for light. Unlike our main interpolation analysis, CM_{EIV} for light in forests showed a substantial negative trend over time ($-0.04 CM_{EIV}$ per decade), CM_{EIV} for moisture showed an overall tendency to increase in grasslands, and temperature showed more pronounced positive trends across habitats (Fig. 4).

DISCUSSION

Widespread nutrient enrichment across Europe

Our study represents the first continent-wide assessment of long-term temporal dynamics in environmental preferences of plants reflected in community composition changes and spanning multiple abiotic gradients simultaneously. Among the environmental conditions assessed

Table 1. Hypothesized directions of temporal changes in EIVs in European plant communities. The sign of the expected change indicates an increase (+) or decrease (–) in EIVs. The table reports the related putative drivers and the ecological processes (species composition changes) through which we expect these drivers to affect CM_{EIVs} .

EIV	Expected change over time	Affected ecosystems	Putative drivers	Ecological processes
Light	+	Forests	Increased overstory disturbance events (e.g., windthrows, drought, and bark beetle outbreaks)	Gains in light-demanding species following canopy openness due to enhanced tree mortality (16, 76)
	–	All	Management cessation; nutrient pollution; CO ₂ fertilization	Gains in species adapted to shadier vegetation and higher above-ground biomass (9, 35, 37, 51)
Temperature	+	Cold and temperate	Global warming	Losses of cold-adapted species and gains in thermophilous species (10, 15, 16, 20)
	–	Temperate and warm, especially forests	Management cessation; nutrient pollution; CO ₂ fertilization	Losses of thermophilous species following cooler microclimatic conditions induced by increased canopy and/or herb-layer density (14)
Moisture	+	Dry	Management cessation	Losses of dry-habitat specialists and gains of mesophilous species (10, 14, 26, 77)
	–	Wet	Increasing drought frequency and land-use change (e.g., soil drainage)	Losses of hygrophilous (wet-adapted) species following lowered water tables (9, 12, 78)
Nitrogen	+	All, especially nutrient-poor	Management cessation; nutrient pollution	Losses of oligotrophic, weakly competitive species and gains of competitive, nutrient-tolerant species following biomass and litter build-up and nutrient enrichment (9–11, 37)
Reaction	+	All	Abatement of ammonia and sulfur emissions (reduced “acid rain”) after 1980s	Gains in less acidophilous species in response to soil pH recovery (18, 51, 79, 80)
	–	All	Ammonia and sulfur emissions (1960–1980s)	Gains in acidophilous species in response to soil acidification caused mainly by sulfur deposition (17, 19)

through bioindication, an increase in nitrogen values has emerged as the strongest and most common trend across European plant communities over the past 60 years. This finding aligns with a substantial body of local and regional resurvey studies that have identified nutrient enrichment and, more broadly, vegetation density and biomass increase (36) as widespread drivers of community composition change across different vegetation types (9–11, 13, 14, 37). We have now confirmed this trend on a continental European scale using an unprecedented amount of data.

The shift toward more nitrogen-demanding plant communities is likely driven, at least in part, by rising nitrogen inputs from cropland fertilization and airborne deposition, which have caused extensive accumulation of reactive nitrogen in European terrestrial ecosystems since the beginning of the 20th century (38, 39). Increases in nitrogen levels are widely recognized as key drivers of shifts in competitive

dynamics of plant communities, favoring generalist and nitrophilous species with efficient nutrient uptake capability over habitat specialists across a variety of habitats (11, 40, 41). Nonetheless, we also acknowledge that the nitrogen indicator value can also partly reflect other related nutrients, such as phosphorus and potassium (42, 43). In addition, nutrient indicator values reflect increases in vegetation density (43, 44) and may, therefore, be driven by factors beyond direct anthropogenic eutrophication, for example, increased atmospheric CO₂ levels (45) and biomass accumulation caused by management cessation (37). Such a confounding effect was corroborated by a concomitant decrease in light conditions (particularly in resurvey plots; Fig. 4 and fig. S2), which reflects an increase in vegetation density and biomass accumulation associated with a decline of light-demanding species. Overall, the near-ubiquitous rise in nitrogen indicator values reflects the combined (and likely interacting) effects of drivers

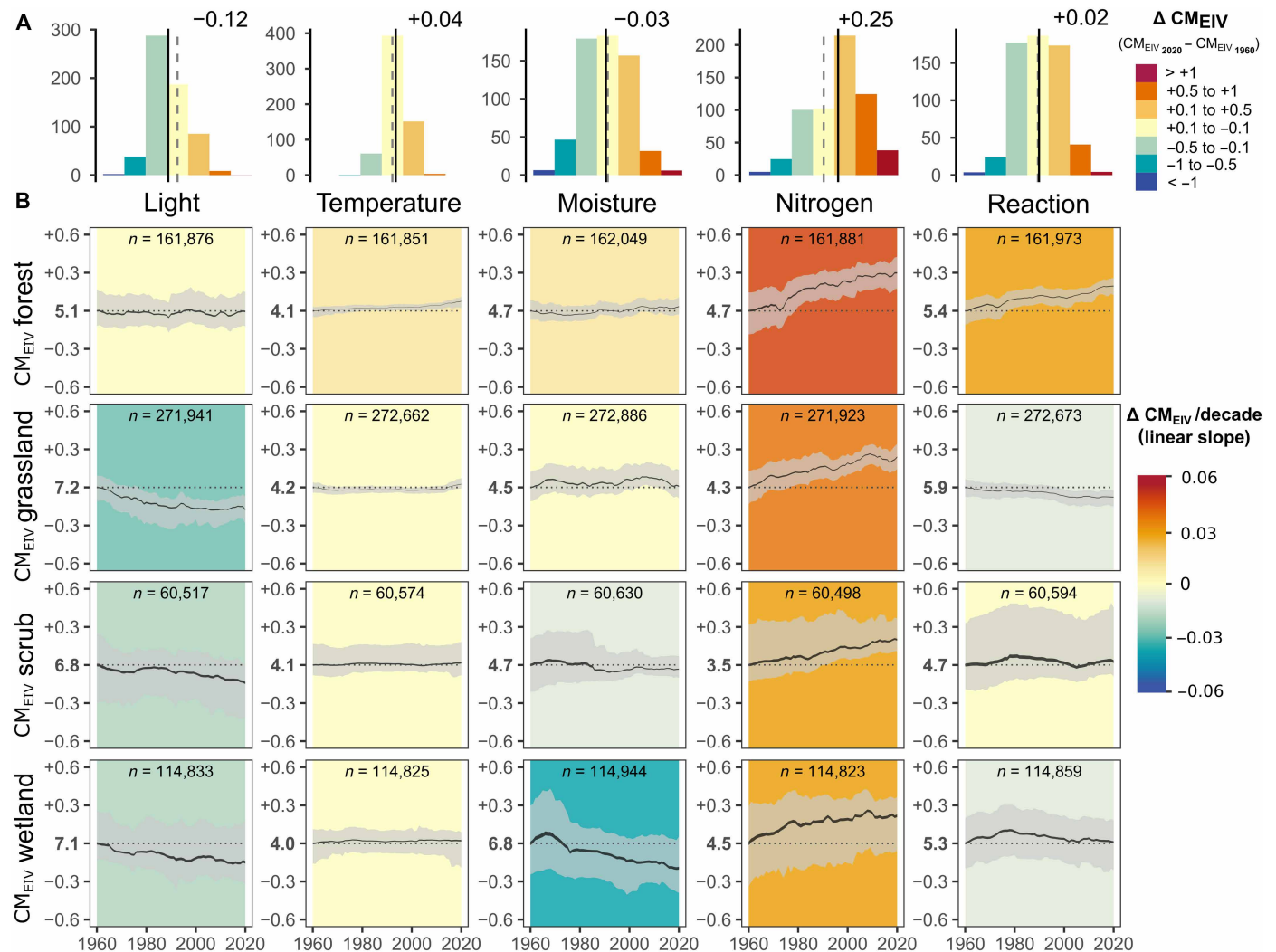


Fig. 1. Interpolated temporal trends of CM_{EIV} across 610,537 European vegetation plots sampled between 1960 and 2020. Histograms in (A) show the distribution of CM_{EIV} changes for the year 2020 compared to 1960; each histogram reports the values of the average CM_{EIV} change across plots (vertical solid line) relative to zero change (vertical dashed line). (B) Temporal trends in average CM_{EIV} s, calculated as the mean CM_{EIV} across plots per year and habitat for each of the 500 decision trees within the random forest model. Trends are summarized as a 95% confidence interval (CI) around the mean (black ribbon) and a prediction interval between the 0.025 and 0.975 quantiles (gray ribbon). Linear regression slopes (background colors) are fitted on the mean predicted values of CM_{EIV} across all plots for each year. The y-axis scale is standardized to the baseline average CM_{EIV} estimated for the year 1960 and displayed in bold. CM_{EIV} s are interpolated using a fixed plot size (225 m² for forests, 16 m² for grasslands, 50 m² for scrub, and 25 m² for wetlands).

promoting higher herb- and shrub-layer biomass productivity and accumulation (43) and is largely consistent with widespread reductions in management intensity across European vegetation (14, 35, 46).

Habitat-specific trends in ecological preferences

We found strong habitat-specific responses for both the magnitude and direction of EIV changes. This finding aligns with previous studies, highlighting the habitat-specific responses of European vegetation to temporal environmental changes (6, 10, 35). While the observed directions of change generally aligned with our expectations (Table 1), habitat-specific trends suggest that some communities may be shifting toward more intermediate indicator values (fig. S1), although this pattern is not consistent across all habitats. For instance, moisture values declined significantly in wetlands (typically harboring

species with higher moisture requirements than other habitats), suggesting the impact of hydrological modifications induced by climate and land-use changes (12). Conversely, moisture increased more in drier and less productive habitats, including Mediterranean scrub and dry grasslands, reflecting an increased prevalence of generalist species adapted to more mesic conditions (10, 47, 48). Likewise, nitrogen EIVs increased most strongly in nutrient-poor habitats, reflecting their higher vulnerability to eutrophication (35, 40, 41), whereas the few fertile habitats showed little or negative changes, as found for woodland clearings and tall forb stands (Fig. 3).

Such contrasting tendencies could partly reflect high species turnover, including the loss of habitat specialists and gains in generalist species affecting various European vegetation types (4, 10, 11). Specifically, an increase in generalist species in the vegetation could shift

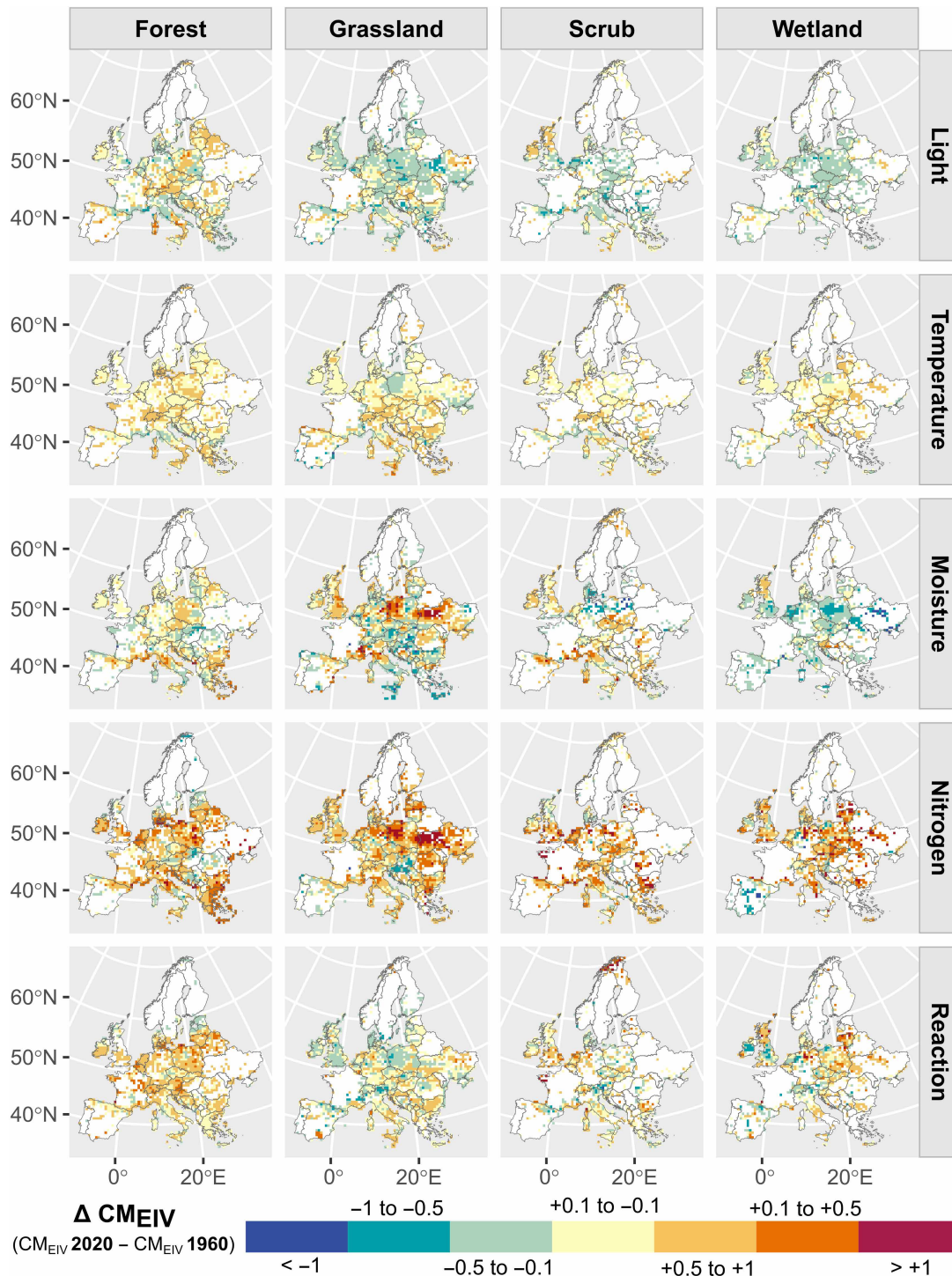
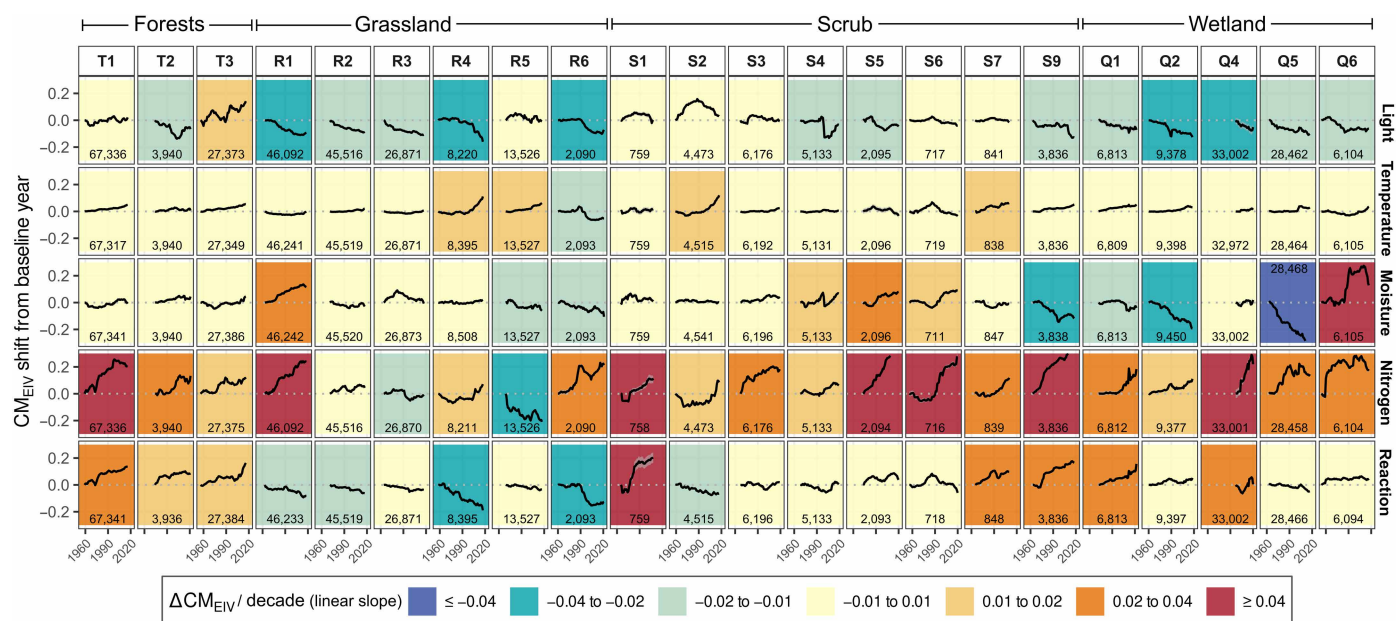


Fig. 2. Geographic patterns in the temporal trends of CM_{EIV} s from 1960 to 2020 across main European habitat types. The maps show the average change in plot-level CM_{EIV} for each EIV variable, aggregated across all plots found within 50-km-by-50-km grid cells. CM_{EIV} values are interpolated using predictions across all plots for the years 1960 and 2020, using a fixed plot size that is representative of the focal habitat (225 m² for forests, 16 m² for grasslands, 50 m² for scrub, and 25 m² for wetlands). Only grid cells containing at least five plots per habitat type sampled within this period are shown. An interactive map at finer resolution is available at http://gmidolo.shinyapps.io/interpolated_EIV_change_app/.



T1 = Broadleaved deciduous forests; **T2** = Broadleaved evergreen forests; **T3** = Coniferous forests; **R1** = Dry grasslands; **R2** = Mesic grasslands; **R3** = Seasonally wet and wet grasslands; **R4** = Alpine and subalpine grasslands; **R5** = Woodland fringes and clearings and tall forb stands; **R6** = Inland salt steppes and salt marshes; **S1** = Tundra; **S2** = Arctic, alpine and subalpine scrub; **S3** = Temperate and Mediterranean-montane scrub; **S4** = Temperate heathland; **S5** = Maquis, arborescent matorral and thermo-Mediterranean scrub; **S6** = Garrigue; **S7** = Spiny Mediterranean heaths; **S9** = Riverine and fen scrub; **Q1** = Raised and blanket bogs; **Q2** = Valley mires, poor fens and transition mires; **Q4** = Base-rich fens and calcareous spring mires; **Q5** = Helophyte beds; **Q6** = Periodically exposed shores

Fig. 3. Interpolated changes in CM_{EIV} s across EUNIS level 2 habitats. Each panel shows temporal trends in average CM_{EIV} s, calculated as the mean CM_{EIV} across plots for each year and habitat type. Linear regression slopes (background colors) express the mean predicted changes in CM_{EIV} every 10 years. The y-axis is standardized to the baseline average CM_{EIV} estimated for the first year of interpolation. To ensure robust temporal coverage and limit extrapolation, interpolated time series for each habitat were restricted to plots sampled between the 0.05 and 0.95 quantiles of sampling years, using a fixed plot size (the habitat-specific median). Estimates are based on models trained on a subset of 384,254 plots, with EUNIS level 2 habitat information included as a predictor. The number of plots for each EUNIS level 2 habitat is shown in each panel.

the CM_{EIV} values toward more intermediate conditions, particularly in habitat types characterized by more extreme conditions (e.g., moisture in wettest or driest habitats, or light in open versus closed-canopy vegetation; Fig. 3). Habitat-dependent trends could also reflect differences in plant strategies and life histories: For example, short-lived pioneer species with higher nitrogen-use efficiency can respond rapidly to environmental change, whereas communities dominated by long-lived perennials may exhibit slower or more constrained CM_{EIV} responses (although removing tree and shrub species did not affect our results in forests and scrub habitats; see fig. S3). From this perspective, differences across habitat types could reflect both ecological change (e.g., habitat degradation) and life-history dependent dynamics of species assemblages along environmental gradients.

The habitat classification system used (49) was developed independently of the EIVs. This independence is crucial for avoiding the influence of the “regression to the mean” (RTM) effect (50), where the response variable artificially shifts toward the mean if subgroups are selected based on extreme values and the time series is limited to only two snapshots (e.g., historical versus modern surveys). In contrast, our analysis relied on long-term time series involving multiple surveys that span the full gradient of environmental conditions across Europe. Furthermore, baseline community-mean indicator values were estimated by interpolating across all plots within a habitat at a given time, rather than relying on individual resurvey comparisons that could be affected by random fluctuations causing RTM (50).

A weak support for a warming trend?

Contrary to our expectations, we did not detect evidence of a temperature increase across most plots and vegetation types based on EIVs. Compared to other putative drivers, our results could suggest that global warming has played a smaller overall role in changes in community indices across all habitat types in Europe so far. This result is consistent with resurvey studies comprising diverse habitats that often found nonsignificant or even negative trends in bioindicated temperature values (14, 37, 48, 51). However, it is likely that global warming could have had indirect effects, mainly by favoring plant biomass buildup and causing increased vegetation density, particularly when coinciding with higher nutrient and CO_2 fertilization effects (45). Furthermore, we cannot definitively exclude a potential direct warming effect, since a marginal increment in temperature values was found in both the interpolation analysis (Fig. 1) and in the time series data (Fig. 4). Unlike nitrogen-related changes, which can trigger rapid species turnover due to the immediate availability of colonizer pools within local habitat mosaics, the response of biological communities to global warming may exhibit lagged and slower dynamics. This is the case for lowlands (52), as temperature gradients in flat terrains often extend over large spatial extents, thus limiting the immediate availability of thermophilous colonizing species nearby and consequently reducing the detectability of warming through bioindication. Conversely, in mountain environments, elevational gradients facilitate more readily observable upward shifts caused by global warming, especially for thermophilous and nutrient-demanding species typically found at lower elevations (53). Our study consistently

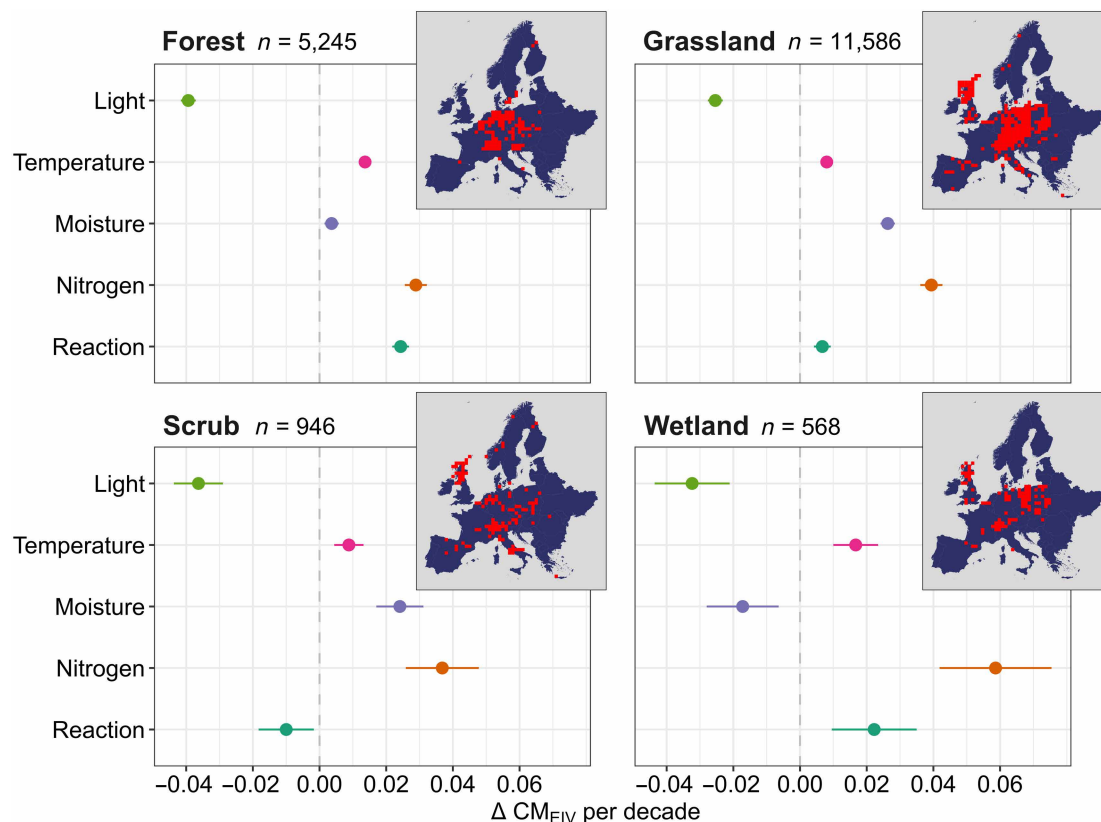


Fig. 4. Trends in CM_{EIVs} modeled across 18,345 resurvey plots collected in the field (ReSurveyEurope) using linear mixed-effect models. Observation records included in the model spanned the period from 1960 to 2020. The main panel shows the estimated slopes (and 95% CI; x axis) representing the change in CM_{EIV} every 10 years for each EIV variable (y axis) and for each main habitat type. The inset maps illustrate the total number and spatial distribution of ReSurveyEurope plot records available for each habitat in Europe in 75-km-by-75-km grid cells.

detected clear warming trends specifically in alpine scrub and grasslands, particularly over the past two decades.

Limitations of EIV-based causal inference

It is important to acknowledge that EIV variables at the species level are partially correlated (fig. S4). At the community level, EIVs exhibited even stronger correlations depending on habitat type (fig. S5). This inherent multicollinearity complicates the straightforward attribution of observed community-mean shifts to distinct putative drivers. Because environmental drivers often act simultaneously, changes over time in one EIV (e.g., nitrogen) are frequently accompanied by correlated shifts in other EIVs (e.g., light or moisture; fig. S2), making it difficult to isolate individual effects. We therefore caution against uncritically drawing direct causal links based solely on EIV variables. A clear example of this challenge can be seen in wetlands: Community changes indicated by shifts in nitrogen were found to be positively correlated with both soil reaction and temperature. This implies that an observed change in a wetland community might be simultaneously signaling a change in soil pH, a warming effect, or a complex combination of both, rather than solely indicating eutrophication. Thus, while the dynamics of different variables serve as proxy indicators and enable the comparison of their potential importance, we emphasize that the interpretation of EIV variables and their observed changes must be made with caution. This further underscores the need for European monitoring

programs to assess local site conditions directly, in addition to biodiversity observation.

Furthermore, we acknowledge that the ecological optima of some species could vary across regions (54) and over long time scales and that such intraspecific variability and potential time-lag responses are not captured by static EIV assignments. However, we expect this limitation to have little influence on our results, because the trends analyzed here primarily reflect changes in species composition at the community level over a few decades. Moreover, any within-species variation in EIVs is averaged across multiple species within each plot, making intraspecific adjustments negligible in the context of our large-scale synthesis.

Environmental implications

Our study provides strong evidence that European plant communities have broadly shifted toward more nitrogen-demanding species composition over the past 60 years. The widespread increase in the prevalence of such species is likely the outcome of several global change drivers that may interact in complex ways, with the specific drivers often varying by context. Furthermore, the trends in light and moisture indicators reinforce the conclusion that land-use change has significantly shaped plant community composition, presumably contributing to habitat deterioration and loss of habitat specialists across various habitat types. Thus, alongside the often-studied effects of global warming (55, 56), eutrophication and land-use management

changes should be accounted for when addressing the impacts of global environmental changes on large-scale dynamics of biological communities.

From a practical standpoint, landscape-planning interventions, such as establishing ecological buffer zones (e.g., hedgerows and road verges) around protected areas in agricultural landscapes, could shield them from nutrient runoff from agricultural fields (57). Nonetheless, reducing nitrogen surpluses at their source, particularly from intensive agriculture and fossil fuel combustion, remains essential to reduce long-range nitrogen deposition and safeguard plant biodiversity across European ecosystems (38). Furthermore, we underscore the need for local conservation and ecological restoration strategies that mitigate soil eutrophication, maintain open vegetation, and preserve characteristic moisture regimes (moist in wet ecosystems and dry in arid ones). These could involve reintroducing or maintaining intermediate disturbance regimes via traditional management practices, such as coppicing (58, 59), litter removal (60), and extensive mowing or grazing (61), or less commonly used management tools for Europe, including prescribed burning (62) and trophic rewinding (63). Coordinated local and policy-level actions are therefore necessary to effectively shape long-term trends in plant community composition change.

MATERIALS AND METHODS

Vegetation plot data

We based our analyses on records of vascular plant species from an initial set of 1,679,403 vegetation plots stored in the EVA (29) and ReSurveyEurope (28) (project no. 222, version 2024-09-19; <https://doi.org/10.58060/hgrb-sw46>). We selected plots with complete information on geographical location, habitat type, plot size, and sampling year, applying specific filters based on each of these variables, as described below. These criteria resulted in a subset of 622,906 vegetation plots in EVA sampled once and 69,487 observations from 21,618 plots in ReSurveyEurope each sampled at least twice. A version including observations from both datasets without temporal replication was used for model training and interpolation. In addition, we used a subset of the ReSurveyEurope dataset to test whether our interpolation approach could predict actual EIV changes within time series data (see “Random forests validation”).

1) Geographic location. We included only plots located in Europe (excluding Iceland, Macaronesia, Svalbard, Russia, and Turkey) with available geographical coordinates (fig. S6). In addition, we excluded plots with a geographic uncertainty greater than 1 km. We retained plots without reported uncertainty, assuming that, in most cases, their true positional error is below this threshold. The coordinates of repeated observations for the same plot in ReSurveyEurope are not always consistent, which can be attributed to relocation errors. Thus, to minimize potential noise in EIV interpolation during model validation, we excluded any plots from ReSurveyEurope where at least one of its survey observations was reported to deviate by more than 100 m from other associated observations for that same plot.

2) Habitat types. Vegetation plots were classified into habitat types using the expert system for the EUNIS Habitat Classification (EUNIS-ESy; version 2021-06-01) (49), which mostly relies on species composition and cover. We focused exclusively on plots categorized as forest, grassland, scrub, and wetland at level 1 of the EUNIS classification. Coastal dune/sandy shore habitats (i.e., “N1”) were reclassified, where possible, into these types based on their physiognomy

(e.g., coastal forests were classified as forest rather than as coastal habitats). Plots from the Danish Nature Database lacking species cover for EUNIS classification were assigned to habitats using the European Union (EU) Habitats Directive’s Annex I habitat conversion (64). In the final selection, the dataset included 181,881 forest, 319,886 grassland, 67,645 scrub, and 122,981 wetland plots.

3) Plot size. We excluded all plots with no information on plot size. We included only plots with sizes ranging from 100 to 1000 m² for forests and from 1 to 100 m² for grasslands, scrub, and wetlands, to exclude outliers and potential reporting errors regarding plot size in EVA and ReSurveyEurope. These plot-size ranges are standard in European vegetation surveys (65) and were explicitly accounted for in the analyses to minimize potential sampling bias.

4) Sampling year. We only included plots sampled between 1945 and 2023. Plots sampled prior to 1945 were excluded due to their much lower number compared to subsequent periods. Although EIV changes were analyzed from 1960 to 2020, the model was calibrated using data from 1945 to 2023. This wider range, analogous to training models over larger geographical extents, potentially enables the model to more robustly capture underlying long-term temporal dynamics by mitigating edge effects at the boundaries of the studied period (1960–2020). The temporal distribution of the included ReSurveyEurope data broadly matched that of the EVA data (fig. S7), and we achieved comprehensive temporal and geographical coverage of plots across most European regions (figs. S8 and S9). For the selected time series within the ReSurveyEurope dataset, the median time span between the first and last observation was 16 years (ranging from 1 to 73 years; SD = 14.6 years).

5) Additional filters on time series data. For the ReSurveyEurope data, plots were excluded if, after applying the previously outlined criteria, all their remaining observations fell within the same year of sampling. The data included both permanent plots (15,856; 73% of these time series), resurveyed at precisely relocated sites, and quasi-permanent plots (5762; 27%), which lacked accurate relocation information. All experimentally manipulated permanent plots were excluded from the ReSurveyEurope dataset.

We provide a summary of the numbers of plots and species used for each methodological step in table S2.

Ecological indicator values

Data on EIVs were sourced from Ecological Indicator Values for Europe (EIVE; version 1.0) (25). This consensus system covers the European flora and was derived from 31 regional, expert-based EIV systems. It contains five ecological indicators, each on a continuous scale from 0 to 10, where 0 represents the lowest and 10 the highest value found on the continent. Because EIVs are on a decimal scale, they can be directly expressed as a percentage of the full European gradient; for instance, a change in mean EIV of 0.1 represents a 1% change of the entire European range for that variable. At least one EIV for light, temperature, soil moisture, soil nitrogen, and soil reaction was available for 13,874 of the 16,810 vascular plant taxa recorded in the selected vegetation plots. The 2936 taxa missing from EIVE were typically very rare in the vegetation plot records (they occurred in 4% of the total number of plots; frequency range: 1 to 1014 plots; mean = 18.2 plots; SD = 53.6 plots), and their exclusion thus had a minimal impact on the results (fig. S10).

We calculated unweighted CM_{EIVs} across all plots for each indicator variable. To account for potentially lower bioindication accuracy due to missing EIVs, we included for each EIV variable only

plots where EIVs were available for at least 80% of the species. This filtering led to the exclusion of only ~1% of plots per EIV variable. On average, the plots retained for analysis had EIVs for more than 98% of the vascular plant species co-occurring in the same plot. In the Supplementary Materials, we report pairwise correlations between EIVs both at the species (fig. S4) and community (plot) level (fig. S5).

We checked the consistency of our approach by comparing our main results (based on CM_{EIV}) with those obtained using the community-weighted mean (CWM_{EIV}), in which mean EIV values are weighted by species cover (abundance) within each plot. Cover values for the same species occurring in different vegetation layers were first merged using the formula proposed by Fischer (66). We then used a subset of 477,990 plots for which species cover data were available and repeated all statistical analyses described below on this subset for both CM_{EIV} and CWM_{EIV} . Since the two approaches yielded very similar results (figs. S11 and S12), we used unweighted community means in the main analyses instead of cover-weighted means, following the principle that less abundant species also reflect environmental conditions (22) and that unweighted means offer more reliable bioindication (67, 68). Last, because long-lived species (such as trees and shrubs) may locally persist after environmental changes, we recalculated CM_{EIV} after excluding 845 tree and shrub species (sourced from <https://floraveg.eu/>) and compared models obtained by excluding such species in forest and scrub vegetation (fig. S3). The results were again very similar, indicating that excluding the longest-living species in closed-canopy vegetation does not meaningfully influence our large-scale patterns.

Random forests training and evaluation

We used random forests (32) to model the dependence of plot-level CM_{EIV} s on space (i.e., elevation, latitude, and longitude) and time (i.e., sampling year) while accounting for the effect of plot size, species richness of vascular plants, and habitat type (either forest, grassland, scrub, or wetland). Tree-based machine learning algorithms, random forests in particular, are well suited to this task (6, 69), as they can model complex interactions among predictors and capture nonlinear, grain-dependent effects more effectively than parametric methods. Prior to modeling, we transformed geographic coordinates to latitude and longitude in meters [using ETRS89/UTM zone 32N (EPSG:25832) projection, hereafter, “northing” and “easting,” respectively] and used this projection throughout the analysis. We extracted elevation at the plot location using a Digital Elevation Model with 90-m horizontal resolution from the European Space Agency (70). We accounted for the effect of vascular plant species richness and plot size (i.e., the species-area relationship) on the response variable (CM_{EIV}), as species-poorer plots are more likely to experience larger changes in CM_{EIV} . For each response variable, we trained our model on 644,524 vegetation plots: 622,906 from EVA and 21,618 from ReSurveyEurope, the latter obtained by selecting one plot observation at random from each time series. The remaining 47,869 plot observations from ReSurveyEurope were excluded from model training but were later used for independent model validation and time series analysis (see “Random forests validation” and “Mixed-effects model analysis on time series data” sections). We also fitted separate models on a subset of 384,254 plots, where EUNIS level 2 habitat information was available. In these models, we used EUNIS level 2 habitat as a predictor instead of broad habitat type. This allowed us to generate predictions that distinguish among

finer habitat categories, for example, separating deciduous from evergreen forests or dry from mesic grasslands.

Analyses were conducted in R (version 4.4.2) (71) using the tidy-models R package collection (72), applying random forests via the ranger engine (33). The dataset was randomly split into training (80%) and test (20%) sets, stratified by CM_{EIV} . Models were fitted using the following formula

$$CM_{EIV} \sim \text{northing} + \text{easting} + \text{elevation} + \text{sampling year} \\ + \text{species richness} + \text{plot size} + \text{habitat type}$$

We included habitat type as a predictor to obtain habitat-specific estimates within a unified model, which improves feature learning in random forests and allows us to compare trends across habitats. We performed hyperparameter tuning with 10-fold cross-validation, testing 24 combinations of the number of randomly sampled predictors (i.e., “mtry” from 2 to 7) and node sizes (2, 5, 10, and 20) with 500 trees. We selected the best set of tuning parameters based on the lowest root mean square error (RMSE) and highest R^2 [i.e., squared Pearson correlation coefficient of observed and predicted data; (72)] (fig. S13).

Model performance was evaluated using a 10-fold cross-validation with three repeats on the training data (table S3) and on the test set (final fit; fig. S14). The models predicted CM_{EIV} with high accuracy, with R^2 ranging from 0.78 (RMSE = 0.62) for nitrogen and 0.93 (RMSE = 0.18) for temperature (table S3). We did not apply block cross-validation (73), as it is not appropriate for interpolation models that use geographic coordinates and time as predictors. In our case, blocking would artificially constrain the model’s ability to learn from continuous spatial and temporal gradients (6). We found no clear spatial pattern in model residuals obtained from the testing data (fig. S15), indicating that the model adequately accounted for spatial patterns in the underlying data and that its predictive accuracy was not systematically biased in any particular region. We assessed variable importance using the node impurity measures from the random forest model (fig. S16).

Random forests validation

To validate our interpolation approach, we assessed its ability to predict changes over time using ReSurveyEurope data, which comprise actual vegetation survey time series collected in the field (6). For each EIV variable, we repeated the model training and testing step 100 times, exclusively on the ReSurveyEurope data. In each iteration, we randomly selected a single observation for each of the 21,618 time series, ensuring that models were trained on data without temporal replication, as in our main analysis (see the “Random forests training and evaluation” section). Model performance was then evaluated on (i) a 20% hold-out test set and (ii) the observed absolute change of CM_{EIV} between the initial and final survey in each time series. A positive correlation in (ii) indicates that CM_{EIV} changes predicted from models trained on data lacking temporal replication reflect actual CM_{EIV} shifts observed across time series data. We obtained good model accuracy, with Pearson correlations between observed and predicted values ranging from 0.51 ($R^2 = 0.26$) for nitrogen and temperature to 0.61 ($R^2 = 0.37$) for moisture (table S4 and fig. S17), indicating that predictions derived from static data capture overall changes in CM_{EIV} .

Interpolating random forests to predict EIV changes

We used the random forests models to predict CM_{EIV} trends from 1960 to 2020 across 610,537 vegetation plots sampled during that

period, keeping all predictors at their original values except for plot size. To account for variability in plot size across habitat types, we set plot size to a fixed representative value for each habitat type when predicting EIVs in space and time: forests (225 m²), grasslands (16 m²), scrub (50 m²), and wetlands (25 m²). Because plot size in EVA and ReSurveyEurope can vary due to differing sampling protocols across contributing databases, the most representative plot sizes mentioned above were determined by calculating the weighted median of the mean plot size from each database, using the number of plots per database as weight. We quantified changes in CM_{EIV}s from 1960 to 2020 by calculating the difference: $\Delta\text{CM}_{\text{EIV}} = \text{CM}_{\text{EIV}2020} - \text{CM}_{\text{EIV}1960}$ (Figs. 1A and 2). We also predicted CM_{EIV}s for each plot and each year across the entire 1960–2020 period, allowing us to summarize continuous temporal trends using partial dependence plots (Figs. 1B and 3), rather than comparing only the endpoints (1960 and 2020). To visualize the geographic patterns of these changes across Europe (Fig. 2), we averaged plot-level $\Delta\text{CM}_{\text{EIV}}$ into 50-km-by-50-km grid cells, incorporating data from all plots and main habitat types within each cell. We also developed a web application in shiny (74) to interactively explore geographic patterns of $\Delta\text{CM}_{\text{EIV}}$ across different habitats and time periods at finer resolution (available at https://gmidolo.shinyapps.io/interpolated_EIV_change_app/).

Mixed-effects model analysis on time series data

To compare conclusions derived from our interpolation approach to those directly computed from actual time series data collected in the field, we also performed a separate analysis of EIV trends exclusively on the ReSurveyEurope data. In this analysis, we used the entire set of 57,255 selected observation records across the 18,345 plots from ReSurveyEurope spanning from 1960 to 2020. We selected all plots that were surveyed at least twice and included all available observations from their time series, rather than limiting comparisons to the initial and final surveys. We restricted the analysis to observations from the same time series that did not experience changes in habitat type (e.g., transitioning from grassland to scrub). This was done to control for plots undergoing rapid changes caused by local land use conversions and plots specifically established to study the successional development of vegetation. We fitted linear mixed-effects models with an identity link function and Gaussian error structure using the lme4 R package (75). For each EIV variable, we modeled the CM_{EIV} using the following lme4 formula

$$\text{CM}_{\text{EIV}} \sim \text{habitat type} \times \text{sampling year} + \log_{10}(\text{plot size}) + (1|\text{dataset/plot})$$

We included an interaction term between habitat type and time (sampling year) to estimate habitat-specific CM_{EIV} change over time. We also accounted for the effect of (log-transformed) plot size (in square meters) and the nested random structure of the plot ID within each dataset ID composing ReSurveyEurope. Before fitting the models, we divided the sampling year by 10 so that the model coefficients represent decadal changes in CM_{EIV}.

Supplementary Materials

This PDF file includes:

Figs. S1 to S17

Tables S1 to S4

REFERENCES

1. P. Jaureguiberry, N. Titeux, M. Wiemers, D. E. Bowler, L. Coscieme, A. S. Golden, C. A. Guerra, U. Jacob, Y. Takahashi, J. Settele, S. Diaz, Z. Molnár, A. Purvis, The direct drivers of recent global anthropogenic biodiversity loss. *Sci. Adv.* **8**, eabm9982 (2022).
2. M. Bernhardt-Römermann, L. Baeten, D. Craven, P. De Frenne, R. Hédl, J. Lenoir, D. Bert, J. Brunet, M. Chudomelová, G. Decocq, H. Dierschke, T. Dirnböck, I. Dörfler, T. Heinken, M. Hermy, P. Hommel, B. Jaroszewicz, A. Keczynski, D. L. Kelly, K. J. Kirby, M. Kopecký, M. Macek, F. Málíš, M. Mirtl, F. J. G. Mitchell, T. Naaf, M. Newman, G. Peterken, P. Petřík, W. Schmidt, T. Standovár, Z. Tóth, H. Van Calster, G. Verstraeten, J. Vladovič, O. Vild, M. Wulf, K. Verheyen, Drivers of temporal changes in temperate forest plant diversity vary across spatial scales. *Glob. Chang. Biol.* **21**, 3726–3737 (2015).
3. M. Dornelas, N. J. Gotelli, B. McGill, H. Shimadzu, F. Moyes, C. Sievers, A. E. Magurran, Assemblage time series reveal biodiversity change but not systematic loss. *Science* **344**, 296–299 (2014).
4. U. Jandt, H. Bruehlheide, F. Jansen, A. Bonn, V. Grescho, R. A. Klenke, F. M. Sabatini, M. Bernhardt-Römermann, V. Blüml, J. Dengler, M. Diekmann, I. Doerfler, U. Döring, S. Dullinger, S. Haider, T. Heinken, P. Horchler, G. Kuhn, M. Lindner, K. Metzner, N. Müller, T. Naaf, C. Peppeler-Lisbach, P. Poschlod, C. Roscher, G. Rosenthal, S. B. Rumpf, W. Schmidt, J. Schrautzer, A. Schwabe, P. Schwartz, T. Sperle, N. Stanik, C. Storm, W. Voigt, U. Wegener, K. Wesche, B. Wittig, M. Wulf, More losses than gains during one century of plant biodiversity change in Germany. *Nature* **611**, 512–518 (2022).
5. M. Vellend, L. Baeten, I. H. Myers-Smith, S. C. Elmendorf, R. Beauséjour, C. D. Brown, P. De Frenne, K. Verheyen, S. Wipf, Global meta-analysis reveals no net change in local-scale plant biodiversity over time. *Proc. Natl. Acad. Sci. U.S.A.* **110**, 19456–19459 (2013).
6. G. Midolo, A. T. Clark, M. Chytrý, F. Essl, S. Dullinger, U. Jandt, H. Bruehlheide, O. Argagnon, I. Biurrun, A. Chiarucci, R. Čuřterevska, P. De Frenne, M. De Sanctis, J. Dengler, J. Divišek, T. Dziuba, R. Ejrnaes, E. Garbolino, E. Illa, A. Jentsch, B. Jiménez-Alfaro, J. Lenoir, J. E. Moeslund, F. Napoleone, R. Pielech, S. B. Rumpf, I. Sanz-Zubizarreta, V. Silva, J. Svenning, G. Swacha, M. Večeřa, D. Vynokurov, P. Keil, Six decades of losses and gains in alpha diversity of European plant communities. *Ecol. Lett.* **28**, e70248 (2025).
7. S. A. Blowes, S. R. Supp, L. H. Antão, A. Bates, H. Bruehlheide, J. M. Chase, F. Moyes, A. Magurran, B. McGill, I. H. Myers-Smith, M. Winter, A. D. Bjorkman, D. E. Bowler, J. E. K. Byrnes, A. Gonzalez, J. Hines, F. Isbell, H. P. Jones, L. M. Navarro, P. L. Thompson, M. Vellend, C. Walldock, M. Dornelas, The geography of biodiversity change in marine and terrestrial assemblages. *Science* **366**, 339–345 (2019).
8. T. Becker, J. Spanka, L. Schröder, C. Leuschner, Forty years of vegetation change in former coppice-with-standards woodlands as a result of management change and N deposition. *Appl. Veg. Sci.* **20**, 304–313 (2017).
9. T. FINDERUP Nielsen, K. Sand-Jensen, H. H. Bruun, Drier, darker and more fertile: 140 years of plant habitat change driven by land-use intensification. *J. Veg. Sci.* **32**, e13066 (2021).
10. K. Klínková, M. G. Sperandii, I. Knollová, J. Danihelka, M. Hájek, P. Hájková, Z. Hroudová, M. Jiroušek, J. Lepš, J. Navrátilová, T. Peterka, P. Petřík, K. Prach, K. Řehounková, J. Rohel, V. Sobotka, M. Vávra, H. Bruehlheide, M. Chytrý, Half a century of temperate non-forest vegetation changes: No net loss in species richness, but considerable shifts in taxonomic and functional composition. *Glob. Chang. Biol.* **31**, e70030 (2025).
11. I. R. Staude, H. M. Pereira, G. N. Daskalova, M. Bernhardt-Römermann, M. Diekmann, H. Pauli, H. Van Calster, M. Vellend, A. D. Bjorkman, J. Brunet, P. De Frenne, R. Hédl, U. Jandt, J. Lenoir, I. H. Myers-Smith, K. Verheyen, S. Wipf, M. Wulf, C. Andrews, P. Barančok, E. Barni, J. Benito-Alonso, J. Bennie, I. Berki, V. Blüml, M. Chudomelová, G. Decocq, J. Dick, T. Dirnböck, T. Durak, O. Eriksson, B. Erschbamer, B. J. Graae, T. Heinken, F. H. Schei, B. Jaroszewicz, M. Kopecký, T. Kudernatsch, M. Macek, M. Malicki, F. Málíš, O. Michelsen, T. Naaf, T. A. Nagel, A. C. Newton, L. Nicklas, L. Oddi, A. Ortman-Ajkai, A. Palaj, A. Petraglia, P. Petřík, R. Pielech, F. Porro, M. Puşcaş, K. Reczyńska, C. Rixen, W. Schmidt, T. Standovár, K. Steinbauer, K. Świerkosz, B. Teleki, J. Theurillat, P. D. Turtureanu, T. Ursu, T. Vanneste, P. Vergeer, O. Vild, L. Villar, P. Vittoz, M. Winkler, L. Baeten, Directional turnover towards larger-ranged plants over time and across habitats. *Ecol. Lett.* **25**, 466–482 (2022).
12. T. Sperle, H. Bruehlheide, Climate change aggravates bog species extinctions in the Black Forest (Germany). *Divers. Distrib.* **27**, 282–295 (2021).
13. I. R. Staude, D. M. Waller, M. Bernhardt-Römermann, A. D. Bjorkman, J. Brunet, P. De Frenne, R. Hédl, U. Jandt, J. Lenoir, F. Málíš, K. Verheyen, M. Wulf, H. M. Pereira, P. Vangansbeke, A. Ortman-Ajkai, R. Pielech, I. Berki, M. Chudomelová, G. Decocq, T. Dirnböck, T. Durak, T. Heinken, B. Jaroszewicz, M. Kopecký, M. Macek, M. Malicki, T. Naaf, T. A. Nagel, P. Petřík, K. Reczyńska, F. H. Schei, W. Schmidt, T. Standovár, K. Świerkosz, B. Teleki, H. Van Calster, O. Vild, L. Baeten, Replacements of small- by large-ranged species scale up to diversity loss in Europe's temperate forest biome. *Nat. Ecol. Evol.* **4**, 802–808 (2020).
14. R. Hédl, M. Kopecký, J. Komárek, Half a century of succession in a temperate oakwood: From species-rich community to mesic forest. *Divers. Distrib.* **16**, 267–276 (2010).
15. B. Richard, J. Dupouey, E. Corcket, D. Alard, F. Archaux, M. Aubert, V. Boulanger, F. Gillet, E. Langlois, S. Macé, P. Montpied, T. Beauflis, C. Begeot, P. Behr, J. Boissier, S. Camaret,

- R. Chevalier, G. Decocq, Y. Dumas, R. Eynard-Machet, J. Gégout, S. Huet, V. Malécot, P. Margerie, A. Mouly, T. Paul, B. Renaux, P. Ruffaldi, F. Spicher, E. Thirion, E. Ulrich, M. Nicolas, J. Lenoir, The climatic debt is growing in the understorey of temperate forests: Stand characteristics matter. *Glob. Ecol. Biogeogr.* **30**, 1474–1487 (2021).
16. J. Kermavnar, L. Kutnar, Three decades of understorey vegetation change in *Quercus*-dominated forests as a result of increasing canopy mortality and global change symptoms. *J. Veg. Sci.* **35**, e13317 (2024).
 17. L. Baeten, B. Bauwens, A. De Schrijver, L. De Keersmaecker, H. Van Calster, K. Vandekerckhove, B. Roelandt, H. Beeckman, K. Verheyen, Herb layer changes (1954–2000) related to the conversion of coppice-with-standards forest and soil acidification. *Appl. Veg. Sci.* **12**, 187–197 (2009).
 18. G. Riofrío-Dillon, R. Bertrand, J. Gégout, Toward a recovery time: Forest herbs insight related to anthropogenic acidification. *Glob. Chang. Biol.* **18**, 3383–3394 (2012).
 19. R. Hédli, Vegetation of beech forests in the Rychlebské Mountains, Czech Republic, re-inspected after 60 years with assessment of environmental changes. *Plant Ecol.* **170**, 243–265 (2004).
 20. M. Gottfried, H. Pauli, A. Futschik, M. Akhalkatsi, P. Barančok, J. L. Benito Alonso, G. Coldea, J. Dick, B. Erschbamer, M. R. Fernández Calzado, G. Kazakis, J. Krajčí, P. Larsson, M. Mallaun, O. Michelsen, D. Moiseev, F. Molau, A. Merzouki, L. Nagy, G. Nakhutsrishvili, B. Pedersen, G. Pelino, M. Puscas, G. Rossi, A. Stanisci, J.-P. Theurillat, M. Tomaselli, L. Villar, P. Vittoz, I. Vogiatzakis, G. Grabherr, Continent-wide response of mountain vegetation to climate change. *Nat. Clim. Chang.* **2**, 111–115 (2012).
 21. R. Hédli, M. Bernhardt-Römermann, J. A. Grytnes, G. Jurassinski, J. Ewald, Resurvey of historical vegetation plots: A tool for understanding long-term dynamics of plant communities. *Appl. Veg. Sci.* **20**, 161–163 (2017).
 22. M. Diekmann, Species indicator values as an important tool in applied plant ecology—A review. *Basic Appl. Ecol.* **4**, 493–506 (2003).
 23. H. Ellenberg, Kausale Pflanzensoziologie auf physiologischer Grundlage. *Ber. d. Deutsch. Bot. Ges.* **63**, 25–31 (1950).
 24. L. Ramensky, I. Tsatsenkin, O. Chizhikov, N. Antipin, *Ekologicheskaya Otsenka Kormovykh Ugodyj Po Rastitel'nomu Pokrovu [Ecological Evaluation of Grazed Lands by Their Vegetation (in Russian)]* (VNIIG, Moscow, 1956).
 25. J. Dengler, F. Jansen, O. Chusova, E. Hüllbusch, M. P. Nobis, K. Van Meerbeek, I. Axmanová, H. H. Bruun, M. Chytrý, R. Guarino, G. Karrer, K. Moeyts, T. Raus, M. J. Steinbauer, L. Tichý, T. Tyler, K. Batsatsashvili, C. Bita-Nicolae, Y. Didukh, M. Diekmann, T. Englich, E. Fernández-Pascual, D. Frank, U. Graf, M. Hájek, S. D. Jelaska, B. Jiménez-Alfaro, P. Julve, G. Nakhutsrishvili, W. A. Ozinga, E. K. Ruprecht, U. Šilc, J. P. Theurillat, F. Gillet, Ecological Indicator Values for Europe (EIVE) 1.0. *Veg. Classif. Surv.* **4**, 7–29 (2023).
 26. C. Lelli, L. Nascimbene, D. Alberti, N. Agostini, A. Zoccola, G. Piovesan, A. Chiarucci, Long-term changes in Italian mountain forests detected by resurvey of historical vegetation data. *J. Veg. Sci.* **32**, e12939 (2021).
 27. S. Boch, H. Küchler, M. Küchler, A. Bedolla, K. T. Ecker, U. H. Graf, T. Moser, R. Holderegger, A. Bergamini, Observer-driven pseudoturnover in vegetation monitoring is context-dependent but does not affect ecological inference. *Appl. Veg. Sci.* **25**, e12669 (2022).
 28. I. Knollová, M. Chytrý, H. Bruelheide, S. Dullinger, U. Jandt, M. Bernhardt-Römermann, I. Biurrun, F. de Bello, M. Glaser, S. Hennekens, F. Jansen, B. Jiménez-Alfaro, D. Kadaš, E. Kaplan, K. Klinská, B. Lenzner, H. Pauli, M. G. Sperandii, K. Verheyen, M. Winkler, O. Abdaladze, S. Acíć, A. T. R. Acosta, A. Alignier, C. Andrews, R. Arlettaz, F. Attorre, I. Axmanová, M. Babbí, L. Baeten, J. Baran, E. Barni, J. L. Benito-Alonso, C. Berg, A. Bergamini, I. Berki, S. Boch, B. Bock, F. Bode, G. Bonari, K. Boublík, A. J. Britton, J. Brunet, V. Bruzzaniti, S. Buholzer, S. Burrascano, J. A. Campos, B. G. Carlsson, M. L. Carranza, T. Černý, K. Charmillot, A. Chiarucci, P. Choler, K. Chytrý, E. Corcket, A. Csecserits, M. Cutini, M. Czarniecka-Wiera, J. Danihelka, M. C. de Francesco, P. De Frenne, M. Di Musciano, M. De Sanctis, B. Deák, G. Decocq, I. Dembic, J. Dengler, V. Di Cecco, J. Dick, M. Diekmann, H. Dierschke, T. Dirnböck, I. Doerfler, J. Doležal, U. Döring, T. Durak, C. Dwyer, R. Ejrnæs, I. Ermakova, B. Erschbamer, G. Fanelli, M. R. Fernández-Calzado, T. Fickert, A. Fischer, M. Fischer, K. Foremnik, J. Frouz, R. García-González, D. García-Magro, I. García-Mijangos, R. G. Gavilán, M. Germ, D. Ghosn, K. Gigauri, J. Gizela, A. Golob, V. Golub, D. Gómez-García, D. Gowing, J. A. Grytnes, B. Güler, A. Gutiérrez-Girón, P. Haase, S. Haider, M. Hájek, M. Halassy, M. Harásek, W. Härdtle, T. Heinken, A. Hester, J. Y. Humbert, R. Ibáñez, E. Illa, B. Jaroszewicz, K. Jensen, A. Jentsch, M. Jiroušek, V. Kalníková, R. Kanka, J. Kapfer, G. Kazakis, J. Kermavnar, S. Kesting, L. Khanina, E. Kindermann, M. Kotrik, T. Koutecký, L. Kozub, G. Kuhn, L. Kutnar, D. La Montagna, A. Lamprecht, J. Lenoir, J. Lepš, C. Leuschner, J. Lorite, B. Madsen, R. M. Ugarte, M. Malicki, T. Maliniemi, F. Málíš, J. A. Maringer, R. Marrs, S. Matesanz, K. Metzke, S. Meyer, J. Millett, R. J. Mitchell, J. E. Moeslund, P. Moiseev, U. M. di Cella, O. Mudrák, F. Müller, N. Müller, T. Naaf, L. Nagy, F. Napoleone, J. Nascimbene, J. Navrátilová, J. M. Ninot, Y. Niui, S. Normand, R. Ogaya, V. Onipchenko, A. Orczewska, A. Ortmann-Ajkai, R. J. Pakeman, I. Pardo, R. Pätzsch, R. K. Peet, J. Penuelas, C. Peppeler-Lisbach, J. Pérez-Hernández, A. Pérez-Haase, A. Petraglia, P. Petřík, R. Pielech, H. Piórkowski, E. Pladevall-Izard, P. Poschod, K. Prach, S. Praleskouskaya, V. Prokhorov, S. Provoost, M. Puşcaş, S. Pustková, C. F. Randin, V. Rašomavičius, K. Reczyńska, T. Rédei, K. Řehounková, N. Richner, A. C. Risch, C. Rixen, S. Rosbakh, C. Roscher, G. Rosenthal, G. Rossi, H. Rötzer, C. Roux, S. B. Rumpf, E. Ruprecht, S. Růsina, I. Sanz-Zubizarreta, M. Schindler, W. Schmidt, D. Schories, J. Schrautzer, H. Schubert, M. Schuetz, A. Schwabe, H. Schwaiger, P. Schwartz, J. Šebesta, H. Seiler, U. Šilc, V. Silva, P. Šmilauer, M. Šmilauerová, T. Sperle, A. Stachurska-Swakoń, N. Stanik, A. Stanisci, K. Steffen, C. Storm, H. G. Strohm, N. Sugorkina, K. Świerkosz, S. Świercz, M. Szymura, B. Teleki, G. Thébaud, J. P. Theurillat, L. Tichý, U. A. Treier, P. D. Turtureanu, K. Ujházy, M. Ujházyová, T. M. Ursu, A. K. Uziębło, O. Valkó, H. Van Calster, K. Van Meerbeek, B. Vandevoorde, V. Vandvik, M. Varricchio, K. Vassilev, L. Villar, R. Virtanen, P. Vittoz, W. Voigt, A. von Hessberg, G. von Oheimb, E. Wagner, G. R. Walther, C. Wellstein, K. Wesche, M. Wilhelm, W. Willner, S. Wipf, B. Wittig, T. Wohlgemuth, B. A. Woodcock, M. Wulf, F. Essl, ReSurveyEurope: A database of resurveyed vegetation plots in Europe. *J. Veg. Sci.* **35**, e13235 (2024).
 29. M. Chytrý, S. M. Hennekens, B. Jiménez-Alfaro, I. Knollová, J. Dengler, F. Jansen, F. Landucci, J. H. J. Schaminée, S. Acíć, E. Agrillo, D. Ambarli, P. Angelini, I. Apostolova, C. Berg, C. Berg, E. Bergmeier, I. Biurrun, Z. Botta-Dukát, H. Brisse, J. A. Campos, L. Carlón, A. Čarni, L. Casella, J. Csiky, R. Čuštvereška, Z. D. Stevanović, J. Danihelka, E. De Bie, P. de Ruffray, M. De Sanctis, W. B. Dickoré, P. Dimopoulos, D. Dubyna, T. Dziuba, R. Ejrnæs, N. Ermakov, J. Ewald, G. Fanelli, F. Fernández-González, Ú. Fitzpatrick, X. Font, I. García-Mijangos, R. G. Gavilán, V. Golub, R. Guarino, R. Haveman, A. Indreica, D. I. Gürsoy, U. Jandt, J. A. M. Janssen, M. Jiroušek, Z. Kacki, A. Kavgaci, M. Kleikamp, V. Kolomyichuk, M. K. Čuk, D. Krstonošić, A. Kuzemko, J. Lenoir, T. Lysenko, C. Marcenò, V. Martynenko, D. Michalčová, J. E. Moeslund, V. Onyshchenko, H. Pedashenko, A. Pérez-Haase, T. Peterka, V. Prokhorov, V. Rašomavičius, M. P. Rodríguez-Rojo, J. S. Rodwell, T. Rogova, E. Ruprecht, S. Růsina, G. Seidler, J. Šibík, U. Šilc, Ž. Škvorc, D. Sopotlieva, Z. Stančík, J. C. Svenning, G. Swacha, I. Tsiropidis, P. D. Turtureanu, E. Uğurlu, D. Uogintas, M. Valachovič, Y. Vashenyak, K. Vassilev, R. Venanzoni, R. Virtanen, L. Weekes, W. Willner, T. Wohlgemuth, S. Yamalov, European Vegetation Archive (EVA): An integrated database of European vegetation plots. *Appl. Veg. Sci.* **19**, 173–180 (2016).
 30. M. D. Mahecha, F. Gans, G. Brandt, R. Christiansen, S. E. Cornell, N. Fomferra, G. Kraemer, J. Peters, P. Bodesheim, G. Camps-Valls, J. F. Donges, W. Dorigo, L. M. Estupinan-Suarez, V. H. Gutierrez-Velez, M. Gutwin, M. Jung, M. C. Londoño, D. G. Miralles, P. Papastefanou, M. Reichstein, Earth system data cubes unravel global multivariate dynamics. *Earth Syst. Dynam.* **11**, 201–234 (2020).
 31. M. Dornelas, A. E. Magurran, S. T. Buckland, A. Chao, R. L. Chazdon, R. K. Colwell, T. Curtis, K. J. Gaston, N. J. Gotelli, M. A. Kosnik, B. McGill, J. L. McCune, H. Morlon, P. J. Mumby, L. Øvreås, A. Studeny, M. Vellend, Quantifying temporal change in biodiversity: Challenges and opportunities. *Proc. Biol. Sci.* **280**, 20121931 (2013).
 32. L. Breiman, Random forests. *Mach. Learn.* **45**, 5–32 (2001).
 33. M. N. Wright, A. Ziegler, ranger: A fast implementation of random forests for high dimensional data in C++ and R. *J. Stat. Softw.* **77**, 1–17 (2017).
 34. L. Lüttger, F. Jansen, R. Kaufmann, G. Seidler, A. Wedler, H. Bruelheide, Linking trends of habitat types and plant species using repeated habitat mapping data. *Appl. Veg. Sci.* **27**, e12799 (2024).
 35. O. Vild, M. Chudomelová, M. Macek, M. Kopecký, J. Prach, P. Petřík, P. Halas, M. Juříček, M. Smyčková, J. Šebesta, M. Vojík, R. Hédli, Long-term shift towards shady and nutrient-rich habitats in Central European temperate forests. *New Phytol.* **242**, 1018–1028 (2024).
 36. R. Buitenwerf, B. Sandel, S. Normand, A. Mimet, J. C. Svenning, Land surface greening suggests vigorous woody regrowth throughout European semi-natural vegetation. *Glob. Chang. Biol.* **24**, 5789–5801 (2018).
 37. G. Bonari, A. Bricca, G. Tomasi, L. Dorigatti, A. Bertolli, D. Andreatta, F. M. Sabatini, M. Di Musciano, F. Prosser, Grassland changes in the Eastern Alps over four decades: Unveiling patterns along an elevation gradient. *Appl. Veg. Sci.* **28**, e70012 (2025).
 38. M. Sutton, C. Howard, J. Erisman, G. Billen, A. Bleeker, P. Grennfelt, H. van Grinsven, B. Grizzetti, *The European Nitrogen Assessment* (Cambridge Univ. Press, 2011).
 39. W. de Vries, M. Posch, D. Simpson, F. A. A. M. de Leeuw, H. J. M. van Grinsven, L. F. Schulte-Uebbing, M. A. Sutton, G. H. Ros, Trends and geographic variation in adverse impacts of nitrogen use in Europe on human health, climate, and ecosystems: A review. *Earth. Sci. Rev.* **253**, 104789 (2024).
 40. R. Bobbink, K. Hicks, J. Galloway, T. Spranger, R. Alkemade, M. Ashmore, M. Bustamante, S. Cinderby, E. Davidson, F. Dentener, B. Emmett, J. W. Erisman, M. Fenn, F. Gilliam, A. Nordin, L. Pardo, W. De Vries, Global assessment of nitrogen deposition effects on terrestrial plant diversity: A synthesis. *Ecol. Appl.* **20**, 30–59 (2010).
 41. G. Midolo, R. Alkemade, A. M. Schipper, A. Benítez-López, M. P. Perring, W. De Vries, Impacts of nitrogen addition on plant species richness and abundance: A global meta-analysis. *Glob. Ecol. Biogeogr.* **28**, 398–413 (2019).
 42. M. Chytrý, M. Hejcman, S. M. Hennekens, J. Schellberg, Changes in vegetation types and Ellenberg indicator values after 65 years of fertilizer application in the Rengen Grassland Experiment, Germany. *Appl. Veg. Sci.* **12**, 167–176 (2009).
 43. A. P. Schaffers, K. V. Šykora, Reliability of Ellenberg indicator values for moisture, nitrogen and soil reaction: A comparison with field measurements. *J. Veg. Sci.* **11**, 225–244 (2000).
 44. M. O. Hill, P. D. Carey, Prediction of yield in the Rothamsted Park Grass Experiment by Ellenberg indicator values. *J. Veg. Sci.* **8**, 579–586 (1997).

45. C. Terrer, R. B. Jackson, I. C. Prentice, T. F. Keenan, C. Kaiser, S. Vicca, J. B. Fisher, P. B. Reich, B. D. Stocker, B. A. Hungate, J. Peñuelas, I. McCallum, N. A. Soudzilovskaia, L. A. Cernusak, A. F. Talhelm, K. Van Sundert, S. Piao, P. C. D. Newton, M. J. Hovenden, D. M. Blumenthal, Y. Y. Liu, C. Müller, K. Winter, C. B. Field, W. Viechtbauer, C. J. Van Lissa, M. R. Hoosbeek, M. Watanabe, T. Koike, V. O. Leshyk, H. W. Polley, O. Franklin, Nitrogen and phosphorus constrain the CO₂ fertilization of global plant biomass. *Nat. Clim. Chang.* **9**, 684–689 (2019).
46. S. Hempel, F. Herzog, P. Batáry, E. Öckinger, E. Knop, The impact of abandonment and intensification on the biodiversity of agriculturally marginal grasslands—A systematic review. *Basic Appl. Ecol.* **88**, 9–18 (2025).
47. K. Klinkovská, M. G. Sperandii, B. Trávníček, M. Chytrý, Significant decline in habitat specialists in semi-dry grasslands over four decades. *Biodivers. Conserv.* **33**, 161–178 (2024).
48. M. Harásek, K. Klinkovská, M. Chytrý, Vegetation change in acidic dry grasslands in Moravia (Czech Republic) over three decades: Slow decrease in habitat quality after grazing cessation. *Appl. Veg. Sci.* **26**, e12726 (2023).
49. M. Chytrý, L. Tichý, S. M. Hennekens, I. Knollová, J. A. M. Janssen, J. S. Rodwell, T. Peterka, C. Marcenò, F. Landucci, J. Danihelka, M. Hájek, J. Dengler, P. Novák, D. Zukal, B. Jiménez-Alfaro, L. Mucina, S. Abdulhak, S. Acíç, E. Agrillo, F. Attorre, E. Bergmeier, I. Biurrun, S. Boch, J. Böllöni, G. Bonari, T. Braslavskaya, H. Bruelheide, J. A. Campos, A. Carni, L. Casella, M. Čuk, R. Čušterevska, E. De Bie, P. Delbosq, O. Demina, Y. Didukh, D. Dítě, T. Dziuba, J. Ewald, R. G. Gavilán, J. C. Gégout, G. P. G. del Galdo, V. Golub, N. Goncharova, F. Goral, U. Graf, A. Indreica, M. Isermann, U. Jandt, F. Jansen, J. Jansen, A. Jašková, M. Jiroušek, Z. Kačvi, V. Kalníková, A. Kavğacı, L. Khanina, A. Y. Korolyuk, M. Kozhevnikova, A. Kuzemko, F. Kůzmič, O. L. Kuznetsov, M. Laiviņš, I. Lavrinenko, O. Lavrinenko, M. Lebedeva, Z. Lososová, T. Lysenko, L. Maciejewski, C. Mardari, A. Mariňšek, M. G. Napreenko, V. Onyshchenko, A. Pérez-Haase, R. Pielech, V. Prokhorov, V. Rašomavičius, M. P. R. Rojo, S. Růsina, J. Schrautzer, J. Šibík, U. Šilc, Ž. Škvorc, V. A. Smagin, Z. Stančić, A. Stanisci, E. Tikhonova, T. Tonteri, D. Uogintas, M. Valachovič, K. Vassilev, D. Vynokurov, W. Willner, S. Yamalov, D. Evans, M. P. Lund, R. Spyropoulou, E. Tryfon, J. H. J. Schaminée, EUNIS Habitat Classification: Expert system, characteristic species combinations and distribution maps of European habitats. *Appl. Veg. Sci.* **23**, 648–675 (2020).
50. L. Mazalla, M. Diekmann, Regression to the mean in vegetation science. *J. Veg. Sci.* **33**, e13117 (2022).
51. M. Dano, V. Jung, G. Thiébaud, S. Chollet, Fifty years of regional-scale vegetation change on Atlantic heathlands. *Biol. Conserv.* **308**, 111210 (2025).
52. R. Bertrand, J. Lenoir, C. Piedallu, G. Riofrío-Dillon, P. de Ruffray, C. Vidal, J.-C. Pierrat, J.-C. Gégout, Changes in plant community composition lag behind climate warming in lowland forests. *Nature* **479**, 517–520 (2011).
53. S. B. Rumpf, K. Hülber, G. Klöner, D. Moser, M. Schütz, J. Wessely, W. Willner, N. E. Zimmermann, S. Dullinger, Range dynamics of mountain plants decrease with elevation. *Proc. Natl. Acad. Sci. U.S.A.* **115**, 1848–1853 (2018).
54. P. Hedwall, J. Brunet, M. Diekmann, With Ellenberg indicator values towards the north: Does the indicative power decrease with distance from Central Europe? *J. Biogeogr.* **46**, 1041–1053 (2019).
55. L. H. Antão, A. E. Bates, S. A. Blowes, C. Waldoock, S. R. Supp, A. E. Magurran, M. Dornelas, A. M. Schipper, Temperature-related biodiversity change across temperate marine and terrestrial systems. *Nat. Ecol. Evol.* **4**, 927–933 (2020).
56. D. E. Bowler, C. Hof, P. Haase, I. Kröncke, O. Schweiger, R. Adrian, L. Baert, H.-G. Bauer, T. Blick, R. W. Brooker, W. Dekoninck, S. Domisch, R. Eckmann, F. Hendrickx, T. Hickler, S. Klotz, A. Kraberg, I. Kühn, S. Matesanz, A. Meschede, H. Neumann, R. O'Hara, D. J. Russell, A. F. Sell, M. Sonnenwald, S. Stoll, A. Sundermann, O. Tackenberg, M. Türkay, F. Valladares, K. van Herk, R. van Klank, R. Vermeulen, K. Voigtländer, R. Wagner, E. Welk, M. Wiemers, K. H. Wiltshire, K. Böhning-Gaese, Cross-realm assessment of climate change impacts on species' abundance trends. *Nat. Ecol. Evol.* **1**, 0067 (2017).
57. J. Holden, R. P. Grayson, D. Berdeni, S. Bird, P. J. Chapman, J. L. Edmondson, L. G. Firbank, T. Helgason, M. E. Hodson, S. F. P. Hunt, D. T. Jones, M. G. Lappage, E. Marshall-Harries, M. Nelson, M. Prendergast-Miller, H. Shaw, R. N. Wade, J. R. Leake, The role of hedgerows in soil functioning within agricultural landscapes. *Agric. Ecosyst. Environ.* **273**, 1–12 (2019).
58. T. Fartmann, C. Müller, D. Poniatowski, Effects of coppicing on butterfly communities of woodlands. *Biol. Conserv.* **159**, 396–404 (2013).
59. R. Hédl, J. Šipoš, M. Chudomelová, D. Ustíněk, Dynamics of herbaceous vegetation during four years of experimental coppice introduction. *Folia Geobot.* **52**, 83–99 (2017).
60. J. Häusler, J. Doua, K. Boublík, J. Doudová, Managing light and nutrients to restore plant diversity in temperate woodlands. *Biol. Conserv.* **306**, 111130 (2025).
61. A. R. Schneider, D. Hering, Effects of extensive grazing and mowing compared to abandonment on the biodiversity of European grasslands: A meta-analysis. *Appl. Veg. Sci.* **27**, e70003 (2024).
62. O. Valkó, P. Török, B. Deák, B. Tóthmérész, Review: Prospects and limitations of prescribed burning as a management tool in European grasslands. *Basic Appl. Ecol.* **15**, 26–33 (2014).
63. C. Bonavent, K. Olsen, R. Ejrnæs, C. Fløjgaard, M. D. D. Hansen, S. Normand, J. Svenning, H. H. Bruun, Grazing by semi-feral cattle and horses supports plant species richness and uniqueness in grasslands. *Appl. Veg. Sci.* **26**, e12718 (2023).
64. European Environment Agency, EUNIS terrestrial habitat classification 2021_1 with crosswalks to Annex I in separate rows (2023).
65. M. Chytrý, Z. Otýpková, Plot sizes used for phytosociological sampling of European vegetation. *J. Veg. Sci.* **14**, 563–570 (2003).
66. H. S. Fischer, On the combination of species cover values from different vegetation layers. *Appl. Veg. Sci.* **18**, 169–170 (2015).
67. G. Ostrowski, S. Aicher, A. Mankiewicz, O. Chusova, I. Dembicz, S. Widmer, J. Dengler, Mean ecological indicator values: Use EIVE but no cover-weighting. *Veg. Classif. Surv.* **6**, 57–67 (2025).
68. A. Saatkamp, N. Falzon, O. Argagnon, V. Noble, T. Dutoit, E. Meineri, Calibrating ecological indicator values and niche width for a Mediterranean flora. *Plant Biosyst.* **157**, 301–311 (2023).
69. C. Mariano, B. Mónica, A random forest-based algorithm for data-intensive spatial interpolation in crop yield mapping. *Comput. Electron. Agric.* **184**, 106094 (2021).
70. European Space Agency, Copernicus GLO-90 Digital Elevation Model, distributed by OpenTopography (2024); <https://doi.org/10.5069/G9028PQB>.
71. R Core Team, R: A language and environment for statistical computing, R Foundation for Statistical Computing, R Foundation for Statistical Computing (2024).
72. M. Kuhn, H. Wickham, Tidymodels: A collection of packages for modeling and machine learning using tidyverse principles (2020); <https://www.tidymodels.org>.
73. D. R. Roberts, V. Bahn, S. Boyce, J. Elith, G. Guillera-Arroita, S. Hauenstein, J. J. Lahoz-Monfort, B. Schröder, W. Thuiller, D. I. Warton, B. A. Wintle, F. Hartig, C. F. Dormann, Cross-validation strategies for data with temporal, spatial, hierarchical, or phylogenetic structure. *Ecography* **40**, 913–929 (2017).
74. W. Chang, J. Cheng, J. Allaire, C. Sievert, B. Schloerke, Y. Xie, J. Allen, J. McPherson, A. Dipert, B. Borges, shiny: Web application framework for R. [Preprint] (2023); <https://CRAN.R-project.org/package=shiny>.
75. D. Bates, M. Mächler, B. Bolker, S. Walker, Fitting linear mixed-effects models using lme4. *J. Stat. Softw.* **67**, 1–48 (2015).
76. D. Scherrer, R. Lüthi, H. Bugmann, J. Burnand, T. Wohlgemuth, A. Rudow, Impacts of climate warming, pollution, and management on the vegetation composition of Central European beech forests. *Ecol. Indic.* **160**, 111888 (2024).
77. M. Rosset, M. Montani, M. Tanner, J. Fuhrer, Effects of abandonment on the energy balance and evapotranspiration of wet subalpine grassland. *Agric. Ecosyst. Environ.* **86**, 277–286 (2001).
78. T. Maliniemi, K. Huusko, L. Muurinen, J. A. Grytnes, H. Tukiaainen, R. Virtanen, J. Alahuhta, Temporal changes in boreal vegetation under 70 years of conservation. *Biodivers. Conserv.* **32**, 4733–4751 (2023).
79. K. Reczyńska, K. Świerkosz, Compositional changes in thermophilous oak forests in Poland over time: Do they correspond to European trends? *Appl. Veg. Sci.* **20**, 293–303 (2017).
80. S. B. Rumpf, A. Buri, S. Grand, C. F. Randin, S. Tesson, C. Cianfrani, A. Guisan, Independent trends of mountain vegetation and soil properties over 40 years of environmental change. *J. Veg. Sci.* **36**, e70006 (2025).

Acknowledgments: We thank all colleagues who sampled vegetation plots in the field or digitized them into the databases used in this work. We are grateful to G. Ortega-Solis for assistance with running the statistical analyses on the high-performance computing cluster. We thank the reviewers for their valuable feedback that improved the manuscript. **Funding:** This study was supported by Czech Science Foundation grant 24-14299L (G.M. and P.K.); Austrian Science Foundation FWF grant I 6578 (A.T.C. and F.E.); European Commission (GA no. 101052342) (M.C., U.J., H.B., J.Di., and M.V.); Technology Agency of the Czech Republic (TA ČR) project S573020008 (M.C., J.Di., and M.V.); German Research Foundation (DFG) project 532411638 (U.J. and H.B.); Swiss National Science Foundation (SNSF) grant 408240_235006 (J.De.); Basque Government grant IT487-22 (I.B.); National Recovery and Resilience Plan (NRRP), Mission 4 Component 2 Investment 1.4—call for tender no. 3138 of 16 December 2021, rectified by decree no. 3175 of 18 December 2021 of the Italian Ministry of University and Research funded by the EU-NextGenerationEU, project code CN_00000033 NBFC, CUP I53D2300580001 (G.B.) and CUP J33C22001190001 (A.C.); European Research Council (ERC) Consolidator grant 101124948 (P.D.F.); Czech Science Foundation grant 23-075335 (J.Do.); Federal Ministry of Education and Research BMBF grant FKZ 031B1067C (A.J.); EU, Principality of Asturias, and SEKUENS Agency GRUPIN grants (B.J.-A.); and Danish National Research Foundation grant DNRF173 (J.-C.S.). **Author contributions:** Conceptualization: G.M. and P.K. Formal analysis: G.M. Funding acquisition: P.K., A.T.C., and F.E. Investigation: G.M. and I.A. Data curation: M.C., F.E., S.D., U.J., H.B., J.De., S.A., O.A., I.B., G.B., A.C., R.C., P.D.F., M.D.S., J.Di., J.Do., T.D., R.E., E.G., A.J., B.J.-A., J.L., J.E.M., F.N., S.B.R., J.-C.S., G.S., I.T., M.V., and D.V. Supervision: P.K. Writing—original draft: G.M. Writing—review and editing: G.M., A.T.C., M.C., F.E., S.D., U.J., H.B., J.De., I.A., S.A., O.A., I.B., G.B., A.C., R.C., P.D.F., M.D.S., J.Di., J.Do., T.D., R.E., E.G., A.J., B.J.-A., J.L., J.E.M., F.N., S.B.R., J.-C.S., G.S., I.T., M.V., D.V., and P.K. **Competing interests:** The authors declare

that they have no competing interests. **Data, code, and materials availability:** All data and code needed to evaluate and reproduce the results in the paper are present in the paper, the Supplementary Materials, and/or the following repositories. The R code and data to reproduce the analysis are available in Zenodo: <https://doi.org/10.5281/zenodo.18625789>. An interactive map exploring interpolated spatiotemporal changes in CM_{EIVS} can be accessed at https://gmidolo.shinyapps.io/interpolated_EIV_change_app. The complete vegetation-plot data (including species records) used in this project are stored within the EVA database repository (<https://doi.org/10.58060/250x-we61>); they can be accessed through a request to the EVA

Coordinating Board (see <https://euroveg.org/eva-database>). The data for the EIVE version 1.0 are available in Dengler *et al.* (25) (<https://doi.org/10.3897/VCS.98324.suppl8>). This study did not generate new materials.

Submitted 6 August 2025

Accepted 6 March 2026

Published 10 April 2026

10.1126/sciadv.aeb2493

Sixty years of plant community change in Europe indicate a shift toward nutrient-rich and denser vegetation

Gabriele Midolo, Adam Thomas Clark, Milan Chytrý, Franz Essl, Stefan Dullinger, Ute Jandt, Helge Bruelheide, Jürgen Dengler, Irena Axmanová, Svetlana Ašů, Olivier Argagnon, Idoia Biurrun, Gianmaria Bonari, Alessandro Chiarucci, Renata Šušterevska, Pieter De Frenne, Michele De Sanctis, Jan Divíšek, Jiří Doležal, Tetiana Dziuba, Rasmus Ejrnæs, Emmanuel Garbolino, Anke Jentsch, Borja Jiménez-Alfaro, Jonathan Lenoir, Jesper Erenskjold Moeslund, Francesca Napoleone, Sabine B. Rumpf, Jens-Christian Svenning, Grzegorz Swacha, Irina Tatarenko, Martin Veřba, Denys Vynokurov, and Petr Keil

Sci. Adv. **12** (15), eab2493. DOI: 10.1126/sciadv.aeb2493

View the article online

<https://www.science.org/doi/10.1126/sciadv.aeb2493>

Permissions

<https://www.science.org/help/reprints-and-permissions>

Use of this article is subject to the [Terms of service](#)

Science Advances (ISSN 2375-2548) is published by the American Association for the Advancement of Science. 1200 New York Avenue NW, Washington, DC 20005. The title *Science Advances* is a registered trademark of AAAS.

Copyright © 2026 The Authors, some rights reserved; exclusive licensee American Association for the Advancement of Science. No claim to original U.S. Government Works. Distributed under a Creative Commons Attribution License 4.0 (CC BY).